

RESEARCH ARTICLE

Open Access



Plasma-derived small extracellular vesicles unleash the angiogenic potential in head and neck cancer patients

Luisa Tengler¹, Julia Schütz¹, Moritz Tiedtke¹, Jadwiga Jablonska², Marie-Nicole Theodoraki³, Katja Nitschke⁴, Christel Weiß⁵, Elena Seiz¹, Annette Affolter¹, Frederic Jungbauer¹, Anne Lammert¹, Nicole Rotter¹ and Sonja Ludwig^{1*} 

Abstract

Background In Head and neck cancer (HNC) angiogenesis is essential for tumor progression and metastasis. Small extracellular vesicles (sEVs) from HNC cell lines alter endothelial cell (EC) functions towards a pro-angiogenic phenotype. However, the role of plasma sEVs retrieved from HNC patients in this process is not clear so far.

Methods Plasma sEVs were isolated on size exclusion chromatography columns from 32 HNC patients (early-stage UICC I/II: 8, advanced-stage UICC III/IV: 24), 12 patients with no evident disease after therapy (NED) and 16 healthy donors (HD). Briefly, sEVs were characterized by transmission electron microscopy (TEM), nanoparticle tracking analysis (NTA), BCA protein assays and Western blots. Levels of angiogenesis-associated proteins were determined using antibody arrays. The interaction of fluorescently-labeled sEVs with human umbilical vein ECs was visualized by confocal microscopy. The functional effect of sEVs on tubulogenesis, migration, proliferation and apoptosis of ECs was assessed.

Results The internalization of sEVs by ECs was visualized using confocal microscopy. Based on antibody arrays, all plasma sEVs were enriched in anti-angiogenic proteins. HNC sEVs contained more pro-angiogenic MMP-9 and anti-angiogenic proteins (Serpin F1) than HD sEVs. Interestingly, a strong inhibition of EC function was observed for sEVs from early-stage HNC, NED and HD. In contrast, sEVs from advanced-stage HNC showed a significantly increased tubulogenesis, migration and proliferation and induced less apoptosis in ECs than sEVs from HD.

Conclusions In general, plasma sEVs carry a predominantly anti-angiogenic protein cargo and suppress the angiogenic properties of ECs, while sEVs from (advanced-stage) HNC patients induce angiogenesis compared to HD sEVs. Thus, tumor-derived sEVs within the plasma of HNC patients might shift the angiogenic switch towards angiogenesis.

Keywords Small extracellular vesicles, Exosomes, Angiogenesis, Head and neck cancer, Plasma, Endothelial cells

*Correspondence:

Sonja Ludwig

Sonja.Ludwig@umm.de

Full list of author information is available at the end of the article



© The Author(s) 2023. **Open Access** This article is licensed under a Creative Commons Attribution 4.0 International License, which permits use, sharing, adaptation, distribution and reproduction in any medium or format, as long as you give appropriate credit to the original author(s) and the source, provide a link to the Creative Commons licence, and indicate if changes were made. The images or other third party material in this article are included in the article's Creative Commons licence, unless indicated otherwise in a credit line to the material. If material is not included in the article's Creative Commons licence and your intended use is not permitted by statutory regulation or exceeds the permitted use, you will need to obtain permission directly from the copyright holder. To view a copy of this licence, visit <http://creativecommons.org/licenses/by/4.0/>.

Background

Head and neck cancers (HNCs) are among the most common tumor entities worldwide (Sung et al. 2021). Frequent tumor locations are the oral cavity, oropharynx and larynx with the majority being Head and Neck squamous cell carcinomas (HNSCC). HNCs are usually advanced at the time of diagnosis, therefore often elude standard oncologic treatments, which results in tumor persistence or recurrence (Johnson et al. 2020). Novel therapeutics, such as anti-PD-1 immunotherapy, have fallen short of expectations with low therapeutic response rates, limiting patient prognosis (Ferris et al. 2016; Whiteside 2018). The identification of mechanisms critical for tumor evasion is urgently needed in order to provide effective therapy and improve the prognosis of HNC patients.

A key feature of solid tumors such as HNCs is their ability to induce angiogenesis. Tumor angiogenesis involves the formation and sprouting of new blood vessels from the vasculature to ensure the supply of oxygen and vital nutrients, especially in advanced tumors (Adams and Alitalo 2007). Angiogenesis is dependent on endothelial cell (ECs) proliferation, migration, and tube formation. While in healthy tissues pro- and anti-angiogenic factors are balanced, in the tumor microenvironment pro-angiogenic factors dominate considerably. One of the crucial factors that trigger the angiogenic switch is the hypoxia created by the growing tumor mass. In this context the expression of the hypoxia-induced factor-1 α (HIF-1 α) transcription factor is increased, which in turn activates several pro-angiogenic factors, such as vascular endothelial growth factor (VEGF) and matrix metalloproteinase 9 (MMP-9) (Bergers and Benjamin 2003). sEVs are nanosized lipid vesicles (30–120 nm) with an endosomal origin and belong to the group of extracellular vesicles (EVs). sEVs are crucial mediators of intercellular communication and can mediate various signaling pathways in the tumor microenvironment (TME). Recently, we have shown that sEVs have a suppressive effect on almost all immune cells, including T cells and NK cells, and serve as a surrogate marker for active HNCs (Ludwig et al. 2017). So far, tumor-derived sEVs (TEV) from HNC cell lines have been reported to contain pro-angiogenic proteins and nucleic acids that stimulate endothelial cells in their proliferation, migration, and ultimately blood vessel formation (Ludwig et al. 2018). Together with other TME-related factors, such as hypoxia and enhanced energy metabolism, angiogenesis provides a good foundation for tumor progression.

So far, little is known about the role of plasma sEVs in angiogenesis. This study provides a deeper insight in the angiogenic potential of sEVs and their potential as diagnostic and prognostic value in HNC.

Materials and methods

Patients

Venous blood was collected from head and neck cancer (HNC, n=32) as well as no evident disease patients (NED, n=12) visiting the Department of Otorhinolaryngology, Head and Neck Surgery of the University Hospital Mannheim from 2019 to 2022 and from healthy donors (HD, n=16). The HNC patients were exclusively patients with squamous cell carcinoma, which will be referred to as HNC patients for simplicity. The study was approved by the local ethics committee (2021-552 und 2019-697N) and all participants signed informed consent before study inclusion. For plasma separation, the blood samples were centrifuged at 2000 g for 10 min at room temperature (RT), aliquoted and frozen at -80°C .

Size-exclusion chromatography

sEVs from plasma were prepared by size exclusion chromatography as previously described by Hong et al. (2016): Briefly, freshly thawed plasma specimens were differentially centrifuged at 2000g for 10 min at RT and at 14,000g for 30 min at 4°C , followed by ultrafiltration (Millipore filter, 0.22 μm). Self-made mini-size-exclusion chromatography columns with 10 mL Sepharose CL-2B (Cytiva, #17-0140-01) gel volume were prepared and 1 mL plasma was loaded and eluted with phosphate-buffered saline (PBS) to retrieve 1 mL fractions. The 4th fraction was collected and used for further studies.

BCA protein assay

The protein content of sEVs was analyzed using PierceTM BCA protein assay (Thermo Fisher Scientific) according to the manufacturer's instructions.

Nanoparticle tracking analysis (NTA)

Nanoparticle tracking analysis (NTA) was performed on ZetaView[®] TWIN (Particle Metrix) to determine the size distribution and concentration of the isolated particles. Freshly isolated plasma sEVs from HNC patients were diluted up to 1:10,000 in PBS and from HD and NED up to 1:2000 in PBS and measured at room temperature (RT). Concentration and size ranges were calculated by ZetaView Software (Particle Metrix Version 8.05.11 SP1 and SP2, Sensitivity 80%, Shutter 100, 11 positions, 2 cycles).

Transmission electron microscopy

Transmission electron microscopy (TEM) of plasma sEVs was performed at the Electron Microscopy Core Facility of Heidelberg University as described previously (Jablonska et al. 2022). For negative staining, freshly prepared sEVs were allowed to adsorb to formvar/carbon-coated copper grids and stained with 3% uranyl acetate.

Micrographs were captured using a JEM1400 transmission electron microscope (JEOL Ltd) with a bottom-mounted 4K CMOS camera (TemCam F416; TVIPS).

Western blots

Plasma sEVs (10 µg) in non-reducing (CD63 only) or reducing sample buffer were separated on 4–20% polyacrylamide gels (Bio-Rad, #4561094) and transferred onto nitrocellulose membranes (Bio-Rad, #1620090). Briefly after blocking, the membrane was incubated with the following primary antibodies overnight at 4 °C: anti-CD63 (Invitrogen, #10628D, 1:250), anti-CD9 (Invitrogen, #10626D, 1:500), anti-TSG101 (Invitrogen, #PA5-31260; 1:500), anti-Grp94 (CST, #2104; 1:1000 in 5% BSA in PBS), anti-ApoA1 (CST, #3350; 1:1000). After washing, HRP-conjugated secondary antibodies (IgG Rabbit anti-Mouse, Invitrogen, #31450, 1:10,000 or IgG Goat anti-Rabbit, Invitrogen, #31460, 1:10,000) were added and incubated for 1 h at RT. The chemiluminescence signal was elicited by SuperSignal™ West Dura™ Chemiluminescence Substrate (Thermo Scientific, #34076) according to the manufacturer's instructions.

Angiogenesis antibody arrays

The relative levels of human angiogenesis-related proteins in sEVs were measured using the Human Angiogenesis Array Kit (R&D Systems Inc.). sEVs (140 µg protein) from 4 HNC patients and 3 HDs were incubated with the array according to the manufacturer's instructions, and the results were analyzed using Image J.

Cell culture

Human umbilical vein cells (HUVEC) were obtained from Gibco (#C0035C, 1 female/ Lot#2044494 and 1 male newborn/Lot#2278504) and cultured in Human Large Vessel Endothelial Cell Basal Medium (Gibco, #M-200–500) with 2% (v/v) Large Vessel Endothelial Supplement (LVES; Gibco, #A14608-01) at 37 °C and 5% CO₂ up to passage 6. For functional assays, LVES was replaced by 2% EV-depleted FBS (Gibco, #A2720801).

Cell proliferation assay

HUVECs (5,000 cells) were co-incubated with 5 µg sEVs per well in a 96-well plate for 24 h. As controls, LVES-containing medium (2% LVES) or PBS (CTRL) was used. MTS cell proliferation assay was performed according to the manufacturer's instructions (Abcam, #ab197010). Briefly, the MTS reagent was added at a dilution of 1:10 and incubated for 3 h. Absorbance was measured at 490 nm with a Tecan Infinite® 200 PRO microplate reader.

Endothelial tube formation

HUVECs (20,000) were placed on top of 100 µL Geltrex® LDEV-Free Reduced Growth Factor Basement Membrane Matrix (Gibco, #A14132-02) in 48-well plates and co-incubated with 10 µg sEVs, LVES or PBS (CTRL). After 8 h, tubules were imaged, using phase contrast microscopy at 2.5× magnification (Axiovert 25 CFL, Carl Zeiss Microscopy). For better visualization, tubules were stained with 2 µg/mL Calcein AM (Invitrogen, #L3224) for 30 min at 37 °C. Tubule length and the number of meshes were analyzed with the Angiogenesis Analyzer developed for the Image J software (Carpentier 2012).

Wound healing

HUVECs were grown to confluence in wells of 48-well plates. Monolayers were scratched using pipet tips and cells were co-incubated in the presence of sEVs (10 µg per well). As controls, PBS (CTRL) or 2% LVES-containing medium was added. After 3-, 6-, 12- and 24-h incubation, the wound was imaged using an Axiovert 25 CFL inverted microscope at 10× magnification. After completion of the assay, HUVECs were fixed with 4% paraformaldehyde, stained with 0.5% crystal violet in distilled water, and subsequently imaged again. Wound closure was analyzed using ImageJ and results are expressed as a percentage of the recovery.

Apoptosis assay

To assess apoptosis of ECs Caspase-Glo® 3/7 (Promega, #G8091) assays were performed. HUVECs were seeded in 96-well-plates at a density of 5,000 cells/well in 100 µL. The cells were immediately treated with 50 µL sEVs (5 µg) in PBS and after 24 h an equal volume of luminescent caspase-3/7 substrate was added and incubated at RT for 1 h. Luminescence was read with a Tecan Infinite® 200 PRO microplate reader. As controls, cells were seeded in an LVES-containing medium or treated with PBS (CTRL).

sEV internalization

Isolated sEVs were labeled with PKH67 membrane-labeling solution (Sigma-Aldrich, #PKH67GL-1KT) according to the manufacturer's instructions. Briefly, 600 µg/ml sEV solution was incubated with 2 µM PKH67 solution for 5 min at RT to stain the vesicles' membrane. Excessive dye was removed by Spin Columns (Invitrogen, #4484449). HUVECs (20,000) were seeded on 8-well-chambered slides (Ibidi, #80826). After 24 h, 10 µg labeled sEVs, labeled PBS or PBS only were incubated in a serum-free medium for 4 h. To wash off sEVs bound to the HUVEC surface, cells were treated with

stripping buffer (14.6 g NaCl, 2.5 mL acetic acid, 500 mL distilled water) for 2 min, followed by extensive washing. Cells were fixed with 4% paraformaldehyde for 20 min at RT, permeabilized with 0.1% Triton X-100 for 3 min and labeled with Phalloidin-iFluor 647 (1:500) and DAPI (1:500) for 1 h. Imaging was performed using a Leica SP5 MP confocal microscope (Leica Microsystems) and the images were processed using ImageJ software. Imaging, processing, and analysis were done under constant settings across all samples.

Statistical analysis

Results were graphed and analyzed using GraphPad Prism (9.4.1) and SAS software (release 9.4), respectively. Kruskal–Wallis tests were used to compare groups regarding non-normally distributed outcomes and ANOVA tests for normally distributed outcomes. In the case of a significant test result post hoc tests have been conducted for pairwise comparisons. Because of the small sample sizes, *p* values have not been corrected for multiple testing (i.e. Bonferroni correction). Quantitative data is presented as mean \pm SD (standard deviation) unless otherwise stated. In general, the result of a statistical test has been considered as statistically significant for *p* less than 0.05. Statistically significant outliers (with *p* < 0.01) detected with the Grubbs' test were excluded.

Results

Clinicopathological characterization of the study participants

The clinicopathological characteristics of patients are summarized in Table 1. In this study, we analyzed 32 HNC patients, 12 patients with no evident disease (NED) and 16 healthy donors (HD). The study cohort was representative of HNC patients with predominantly male patients and a median age of 64 years. HDs were age- (median age 54 years) and gender-matched (56% male, 44% female). All patients and HDs were Caucasian. The tumor subsets were in decreasing frequency in the oropharynx, oral cavity, larynx, and hypopharynx. Infection with human papillomavirus, detected by p16 positivity in immunohistochemistry, was prevalent in 39% of tested HNC patients. Regarding other risk factors, the majority of patients smoked tobacco (82%) and/or consumed alcohol (71%). In this study, about half of the patients had large tumors (T3/4). Most tumors spread to lymph nodes ($N > 0$: 70%) with no evidence of distant metastases (M0: 100%) at the time of diagnosis. According to the 8th edition of UICC classification, most patients were diagnosed with advanced stage HNC (UICC III/IV: 70%). Therapy regimens of patients comprised surgery (16%), surgery

with adjuvant (chemo)radiation (59%), primary chemoradiation (18%) and palliative radiotherapy (7%).

Characterization of sEVs

The isolated plasma sEVs were characterized for their morphology by transmission electron microscopy (TEM), for the particle concentration and size distribution by nanoparticle tracking analysis (NTA), and for the particle concentration and protein content by BCA assay and Western blots, respectively.

TEM confirmed a spherical morphology of the isolated sEVs (Fig. 1A). Using NTA, sEVs from HNC patients (1.24×10^{11} particles/mL) revealed higher concentrations than NED and HD sEVs (NED: 3.11×10^{10} , HD: 4.62×10^{10} particles/mL), while median sizes were comparable (Fig. 1B, C). Protein levels of sEVs from HNC (60.8 ± 22.9 μ g/mL) and NED (61.6 ± 17.6 μ g/mL) were elevated compared to HD (49.8 ± 13.8 μ g/mL) (Fig. 1D).

Western blots confirmed the presence of vesicle-associated proteins, i.e. the tetraspanins (CD9 and CD63), and TSG101. Besides, the absence of cellular components such as Grp94 was confirmed and lipoproteins like ApoA1 were shown to be reduced (Fig. 1E, Additional file 2: Fig. S1).

Plasma sEVs contain pro- and anti-angiogenic proteins

To reveal the angiogenic protein profiles of the sEVs, sEV proteomes from HNC patients and HDs were assessed using antibody arrays and compared for their pro- and anti-angiogenic features (Fig. 2).

Overall, antibody arrays showed enrichment in anti-angiogenic proteins, such as platelet factor 4, serpin F1 and thrombospondin-1, compared to pro-angiogenic proteins in all plasma sEVs (Fig. 2B). Furthermore, HNC sEVs contain four times more pro-angiogenic MMP-9, double the amount of dual-function pentraxin-3 and dipeptidyl peptidase IV (DPPIV) is increased by 63% compared to HD sEVs. Besides, anti-angiogenic serpin F1 is more than twice as high in HNC compared to HD sEVs (Additional file 1: Table S1).

Plasma sEVs are internalized by HUVECs and modulate their function

To visualize the interaction of the isolated sEVs with ECs, sEVs were dyed with PKH67, incubated with human umbilical vein endothelial cells (HUVECs) and confocal microscopy was performed after 4 h. As a control, identically stained PBS without sEVs was used (Fig. 3). Internalization of PKH67-stained vesicles by ECs was observed after only 4 h. To analyze the effect of sEVs on the EC function, vesicles from HNC, NED patients or HDs were incubated with HUVECs. Large vessel

Table 1 Clinicopathological characteristics of the patients

	HNC (n = 32)		NED (n = 12)		All (n = 44)	
	n	%	n	%	n	%
Age						
Median	62.5		66		64	
Sex						
Male	20	62.5	6	50	26	59.1
Female	12	37.5	6	50	18	40.9
Tumor site						
Oropharynx	19	59.4	5	41.7	24	54.5
Oral cavity	6	18.8	1	8.3	7	15.9
Larynx	3	9.4	5	41.7	8	18.2
Hypopharynx	4	12.5	1	8.3	5	11.4
HPV status ⁺						
Negative	18	56.3	1	8.3	19	43.2
Positive	8	25.0	4	33.0	12	27.3
n/a	6	18.8	7	58.3	13	29.5
Smoking						
Never	3	9.4	1	8.3	4	9.1
Former	9	28.1	4	33.3	13	29.5
Current	19	59.4	4	33.3	23	52.3
n/a	1	3.1	3	25.0	4	9.1
Alcohol consumption						
Never	4	8.8	0	0	4	9.1
Former	8	26.5	6	50.0	14	31.8
Current	15	44.1	1	8.3	16	36.4
n/a	5	20.6	5	41.7	10	22.7
Tumor size						
T1	2	6.3	4	33.3	6	13.6
T2	14	43.8	4	33.3	18	40.9
T3	9	28.1	1	8.3	10	22.7
T4	7	21.9	3	25.0	10	22.7
Lymph node status						
N0	9	28.1	4	33.3	13	29.5
N1	8	25.0	5	41.7	13	29.5
N2	9	28.1	2	16.7	11	25.0
N3	6	18.8	1	8.3	7	15.9
Metastases						
M0	32	100	12	100	44	100
UICC stages [*]						
I	4	12.5	3	25.0	7	15.9
II	4	12.5	2	16.7	6	13.6
III	9	28.1	4	33.3	13	29.5
IV	15	46.9	3	25.0	18	40.9
Therapy						
Surgery	4	12.5	3	25.0	7	15.9
Surgery plus CRT	14	43.8	5	41.7	19	43.2
Surgery plus RT	6	18.8	1	8.3	7	15.9
Primary CRT	5	15.6	3	25.0	8	18.2
Palliative RT	3	9.4	0	0	3	6.8
Time between end of therapy and sample collection						

Table 1 (continued)

	HNC (n = 32)	NED (n = 12)	All (n = 44)
<6 months		3	25.0
>6 months		3	25.0
>2 years		6	50.0

n number of patients, CRT chemoradiotherapy, RT radiotherapy, +p16 positivity, *International Union Against Cancer (UICC) classification 8th edition

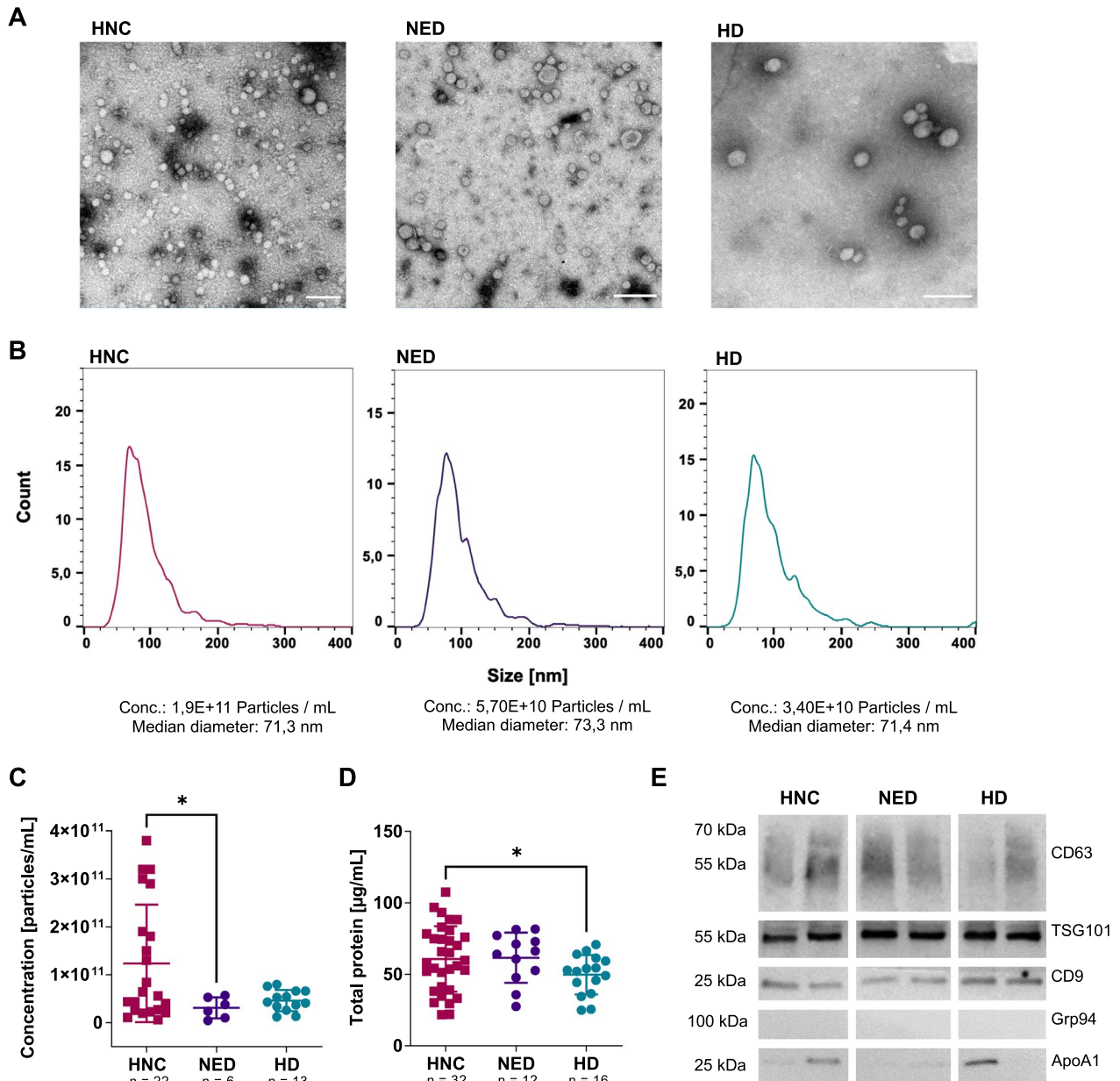


Fig. 1 Characterization of plasma sEVs. sEVs were freshly isolated from plasma of HNC, NED patients and HD by size-exclusion chromatography and characterized for their morphology, particle concentration and protein content. **A** Representative TEM images of sEVs from HNC, NED patients and HD are shown (magnification = 25.000x, scale = 100 nm). **B** Size distribution, concentration and median diameter of the particles were detected using NTA. **C** NTA particle concentration of HNC, NED patients and HD were visualized by scatter plots. **D** Comparison of total protein content in 1 mL of isolated sEVs measured by BCA protein assays. **E** Western blots were performed using 10 µg protein and the presence of typical vesicle proteins CD9, CD63 and TSG101 and the absence of contaminating proteins (Grp94, ApoA1) were shown. P values below 0.05 were considered as significant (*p < 0.05)

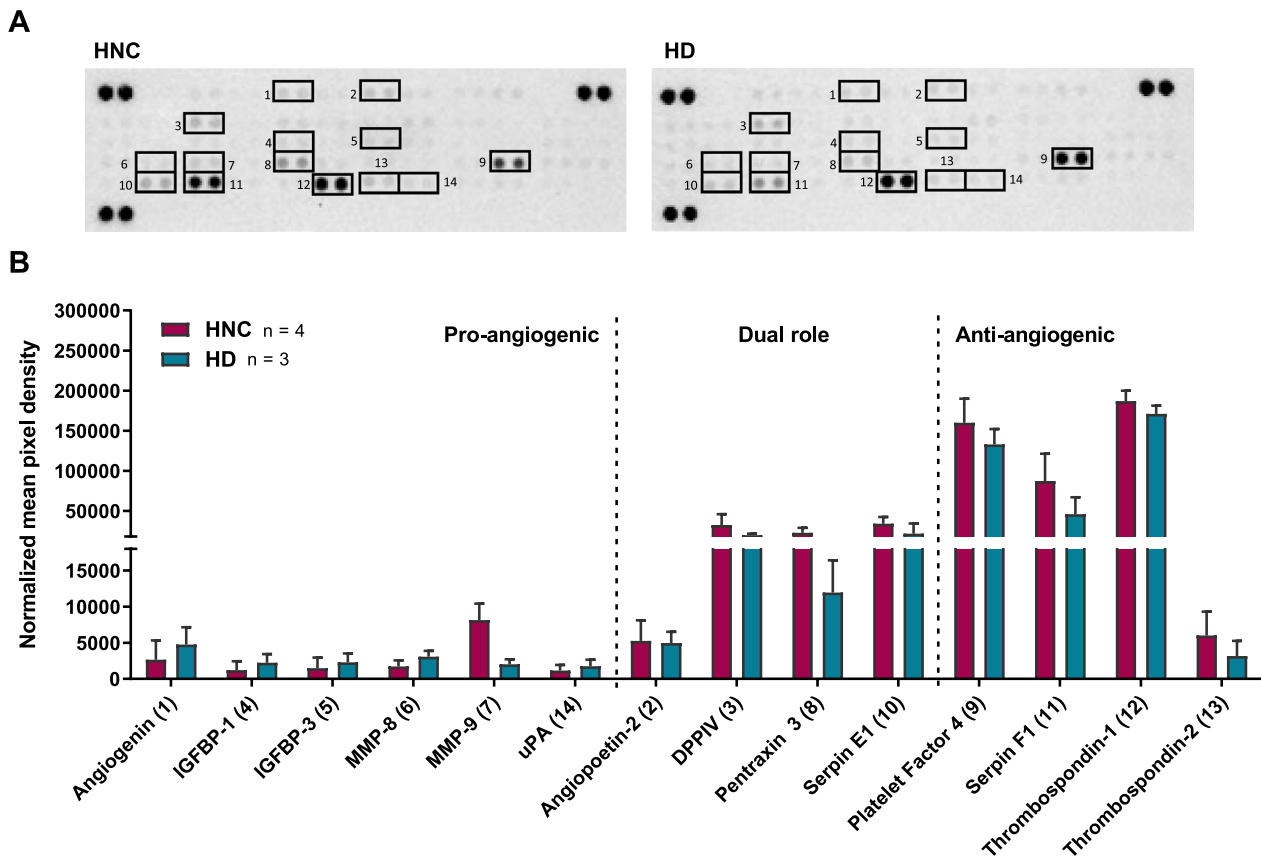


Fig. 2 Relative content of angiogenesis-associated proteins. The angiogenesis antibody arrays were used to measure the angiogenic profile of 140 μ g total protein of the prepared sEVs from HNC patients and healthy donors. The pixel density of each spot was evaluated using ImageJ. **A** Representative images of angiogenesis antibody arrays of one HNC patient and one HD are shown. **B** Column bar graph summarizes the protein levels of angiogenesis-associated markers of sEVs from HNC patients and HDs. Data are shown as means \pm SEM (standard error of the mean)

endothelial supplement (LVES), which contains pro-angiogenic factors like epidermal growth factor (EGF) and basic fibroblast growth factor (bFGF), was used as a positive control and PBS as a negative control (Fig. 4). The effective amount of sEVs was titrated (Additional file 3: Fig. S2).

Interestingly, crystal violet staining showed that after incubation with sEVs (Fig. 4), ECs underwent a morphological change, in which the cells elongated and partially detached, whereas in the control images (PBS or LVES), the cells retained their cobblestone-like arrangement. Next, to investigate the impact of sEVs on the wound healing capacity of HUVEC, a confluent monolayer of cells was wounded mechanically and the regeneration of the cell layer was monitored (Fig. 5A, B). After 24 h, the regeneration of the cell layer was induced by LVES and plasma sEVs, but not by the PBS control (CTRL). The reduction of wound healing by plasma sEVs correlated with the disease activity of the HNC patients or HDs, i.e. sEVs from HDs, NED and early-stage HNC patients

showed a stronger inhibition than sEVs from advanced-stage HNC patients.

Furthermore, tube formation assays were performed to examine the effect of sEVs on the tubulogenesis of HUVECs. HUVECs were seeded on a basement membrane matrix, treated with sEVs and tube formation was monitored every 2 h (Fig. 5C, D). Overall, ECs treated with sEVs formed smaller and less defined networks. As expected, the LVES-containing medium increased the total length of tubules, whereas sEVs from HNC, NED and HD plasma reduced them. Of note, late-stage HNC sEVs appeared to increase the number of developed meshes compared to the other groups.

Next, we assessed the EV-mediated effect on HUVEC proliferation. To this end, sEVs, LVES-containing medium or PBS (CTRL) were added and the proliferation was assessed after 24 h using colorimetric MTS assays. The assay (Fig. 6A) shows that the relative proliferation of ECs was inhibited most by HD, NED and HNC stage I/II sEVs, while the suppression by sEVs from advanced-stage HNCs (UICC III/IV) was less.

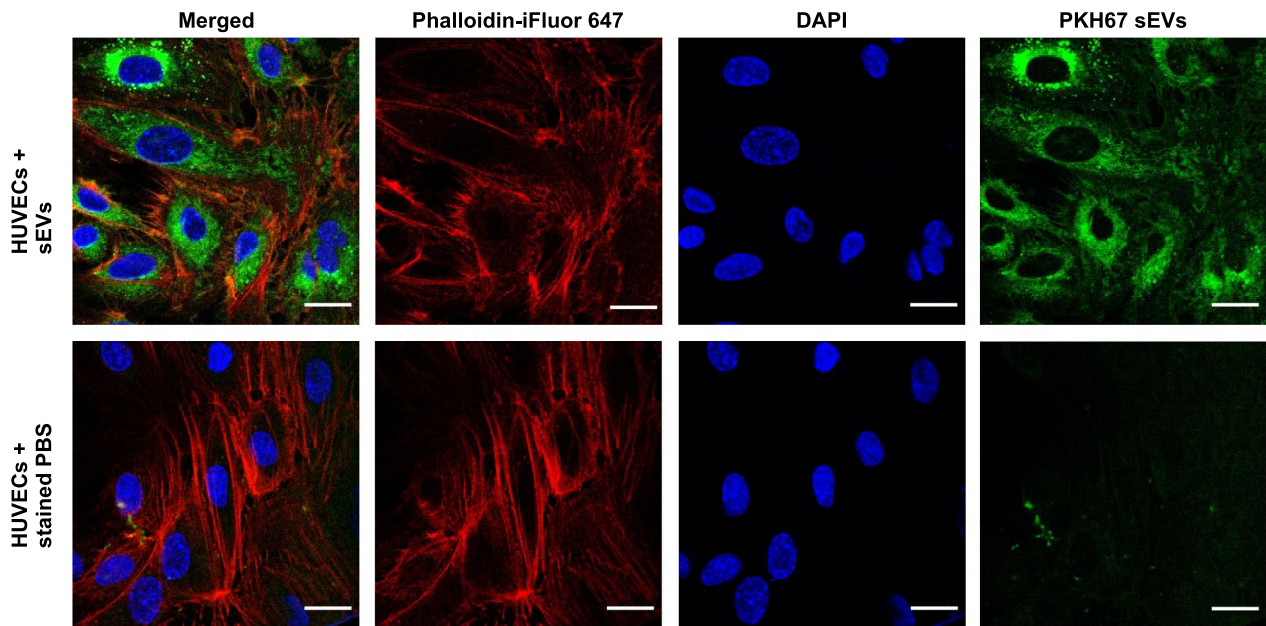


Fig. 3 Plasma sEVs are internalized by HUVECs. Confocal microscopy of HUVECs after 4 h incubation with 20 µg PKH67-stained sEVs (upper row) or stained PBS as control (lower row). Magnification = 40x, scale = 20 µm

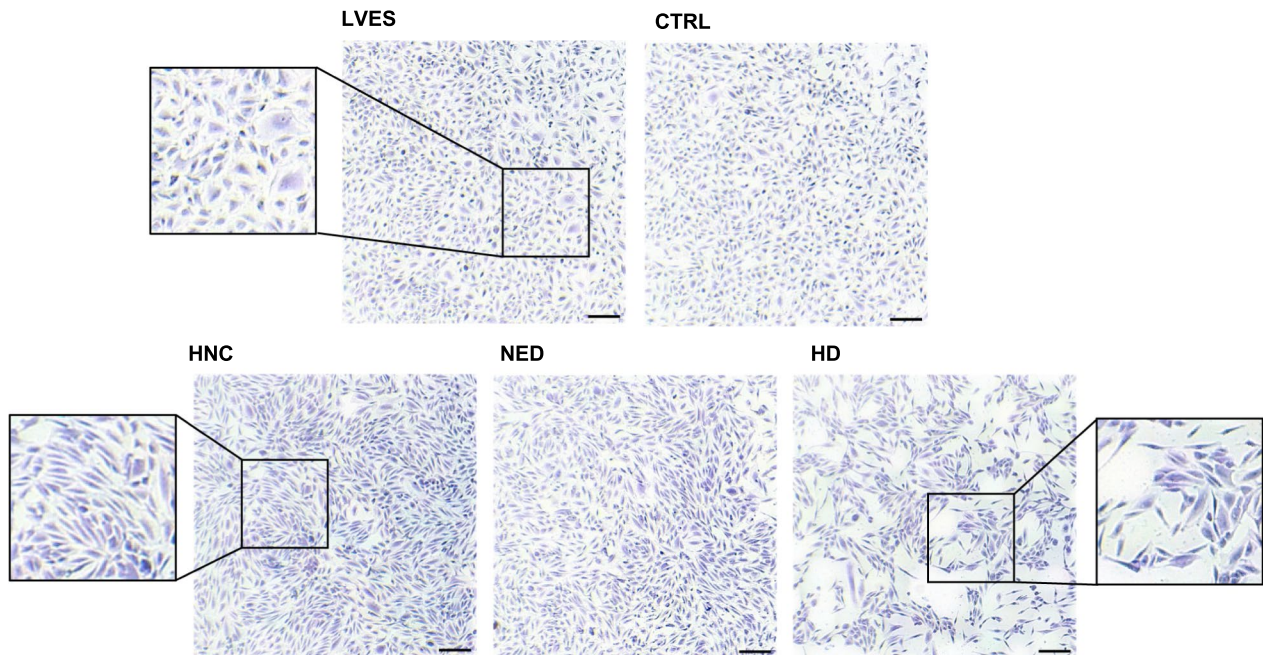


Fig. 4 Crystal violet staining of HUVECs co-incubated with sEVs. Crystal violet staining of HUVECs after 24 h of stimulation with sEVs from HNC, NED patients and HD. HUVECs co-incubated with sEVs from HNC patients showed a rather elongated morphology and remained confluent compared to HUVECs with HD sEVs. The control images, HUVECs with PBS (CTRL) and LVES, visualized cobblestone-shaped and attached cells. Magnification = 2.5x, scale = 200 µm

Since cell detachment was observed after treatment in previous assays, apoptosis of endothelial cells was investigated by measuring caspase 3/7 activity (Fig. 6B). Caspase 3/7 was induced in HUVECs co-incubated with sEVs from HD, NED and early stage HNCs (UICC I/II), while sEVs from advanced stage HNCs did not induce apoptosis of HUVECs (comparable to CTRL/PBS).

All in all, in this manuscript we have found that plasma sEVs inhibit proliferation, migration and tube formation and promote apoptosis of endothelial cells. However, this adverse effect decreases with disease activity and higher tumor stages. Other clinical factors like HPV status, tumor site as well as gender and age had no influence on the angiogenic effect of sEVs on HUVECs (Additional file 4: Fig. S3, Additional file 5: Fig. S4, Additional file 6: Fig. S5, Additional file 7: Fig. S6).

Discussion

A sufficient blood supply is indispensable for cancer growth, progression, and metastasis, and as such defines angiogenesis as one of the hallmarks of cancer (Hanahan and Weinberg 2011). While angiogenesis mediated by TEV from HNC cell lines has been reported to have strong pro-angiogenic potential (Ludwig et al. 2018, 2020a), the angiogenic properties of plasma sEVs from HNC patients have not been examined in detail. Our data indicate that plasma sEVs from HDs have strong anti-angiogenic properties. Compared with HD sEVs, sEVs from NED or HNC patients have pro-angiogenic activities that increase with higher disease activity and advanced tumor stages.

A closer examination of the sEV protein profile reveals mainly the abundance of anti-angiogenic proteins in sEVs from both: HNC patients and HDs. The anti-angiogenic thrombospondin-1 is known to inhibit migration, proliferation, survival, and to promote apoptosis of ECs by directly binding to CD36 and antagonizing the activity of VEGF (Lawler and Lawler 2012). However, recently Liu et al. showed that thrombospondin-1 induced PD-L1 mediated immunosuppression in osteosarcoma resulting in increased tumor growth (Liu et al. 2022), a mechanism that has been described for HNC as well (Ludwig et al. 2017). Besides, platelet factor 4 and serpin F1 have strong anti-angiogenic functions mainly through inhibition of VEGF receptor signaling (Pilatova et al. 2013; Liu

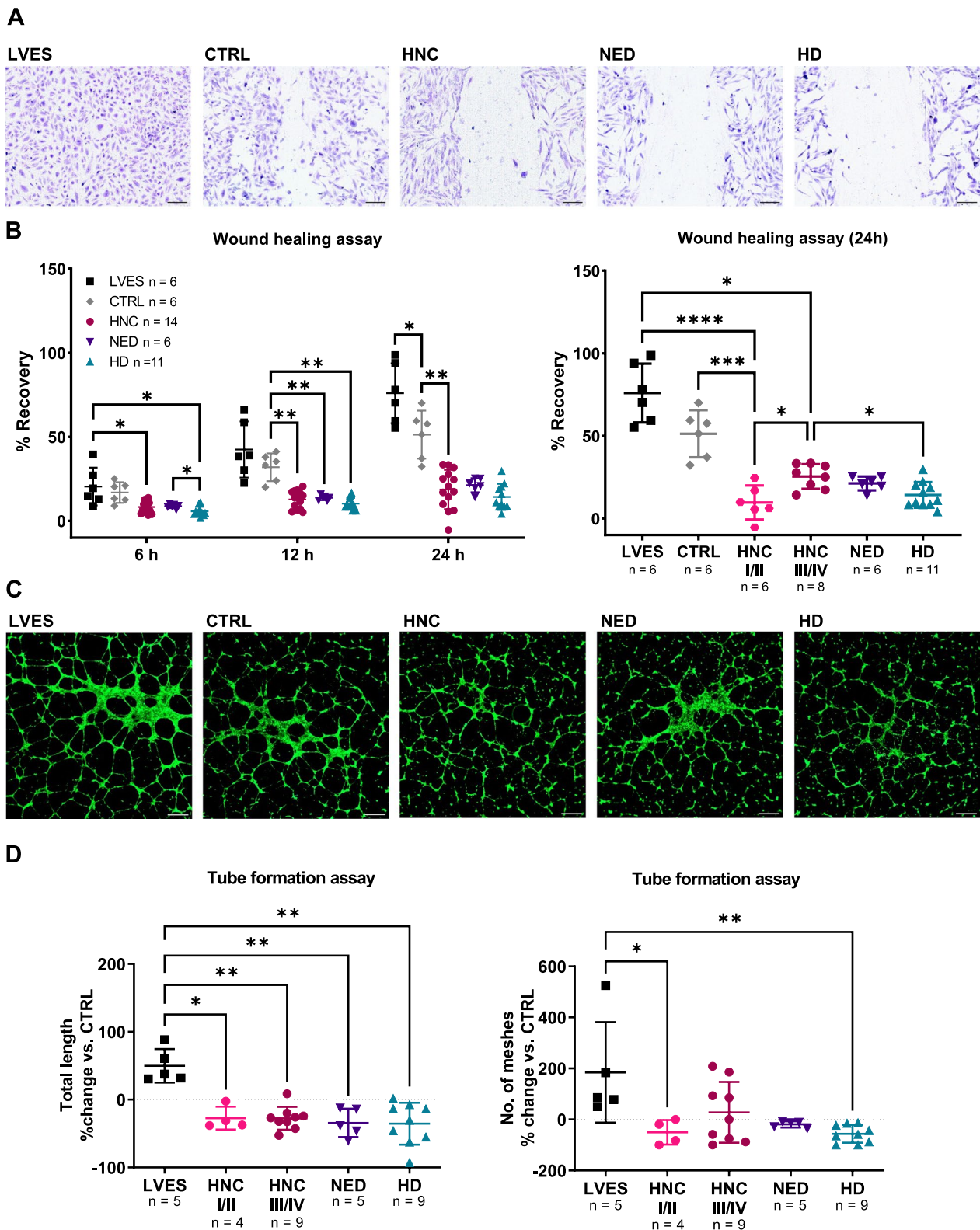
et al. 2005; Dawson et al. 1999). Thus, the observed anti-angiogenic effect of plasma sEVs on ECs is not surprising. Interestingly, in sEVs from HNC patients, the level of pro-angiogenic MMP-9 is increased in comparison to HD. Notari et al. reported that MMP-9 degrades the extracellular matrix (ECM) and basement membrane and activates cytokines promoting angiogenesis, invasion and metastasis by induction of VEGF (Bergers et al. 2000). Additionally, during hypoxia, MMP-9 proteolytically degrades the anti-angiogenic serpin F1 (Notari et al. 2005). MMP-9 is an unfavorable prognostic factor in HNC (Vicente et al. 2005; Liu et al. 2010), bladder cancer (Miao et al. 2017) and ovarian cancer (Jia et al. 2017), which might indicate its key role in angiogenesis.

The internalization of sEVs by ECs and other target cells mediates angiogenesis and immunosuppression in carcinogenesis (Whiteside 2016). Here, we observed the internalization of PKH-dyed sEVs by ECs after 4 h. PKH-dye has been reported to bind non-specifically to lipoproteins (Ludwig et al. 2020a; Lawler and Lawler 2012), our study is supported by others confirming the uptake of PKH-labeled HNC TEV by ECs mainly via receptor-mediated endocytosis after 2–4 h (Ludwig et al. 2018; Pužar Dominkuš et al. 2018).

Crystal violet staining showed a change in cell morphology with elongated fibroblast-like cells and increased cell detachment, which may indicate changes in function and promotion of apoptosis caused by sEV stimulation. The spindle-shaped morphology could also point to an endothelial-to-mesenchymal transition (EndMT), which has been reported for melanoma-derived sEVs (Yeon et al. 2018) and also as a result of MMP-9 stimulation within the endothelial cells (Zhao et al. 2016). Interestingly, the functional effect of sEVs on ECs was stage-dependent: Advanced-stage sEVs induced a better wound recovery, less suppression of proliferation and reduced apoptosis of ECs than sEVs from early-stage HNC, NED or HD. However, the functional impact of sEVs on tubulogenesis is controversial: Some advanced-stage HNC sEVs increased the number of meshes compared to the control but not the total length of the tubules, while HD sEVs showed the strongest inhibition of tube formation. Endothelial cell migration and proliferation are essential for angiogenesis and are regulated by cytokines such as VEGF, bFGF, angiopoietins, and

(See figure on next page.)

Fig. 5 Functional wound healing and tube formation assays of HUVECs co-incubated with sEVs. HUVECs were grown to confluence and mechanically wounded to detect the recovered area in the presence of sEVs. **A** Representative images of migration assays after 24 h of co-incubation with sEVs are visualized by inverted microscopy (magnification = 10x, scale = 150 μ m). **B** The scatter plots present the recovered area in percent of the measured gap after 24 h from scratching. **C** Representative fluorescence microscopy images of tube formation assays after 8 h co-incubation of HUVECs and sEVs. LVES-containing medium was used as a positive control. Magnification = 2.5x, scale = 200 μ m D Scatter plots display the modification of total tube length and number of meshes compared to the PBS control (dotted line). * $p < 0.05$; ** $p < 0.01$; *** $p < 0.001$; **** $p < 0.0001$



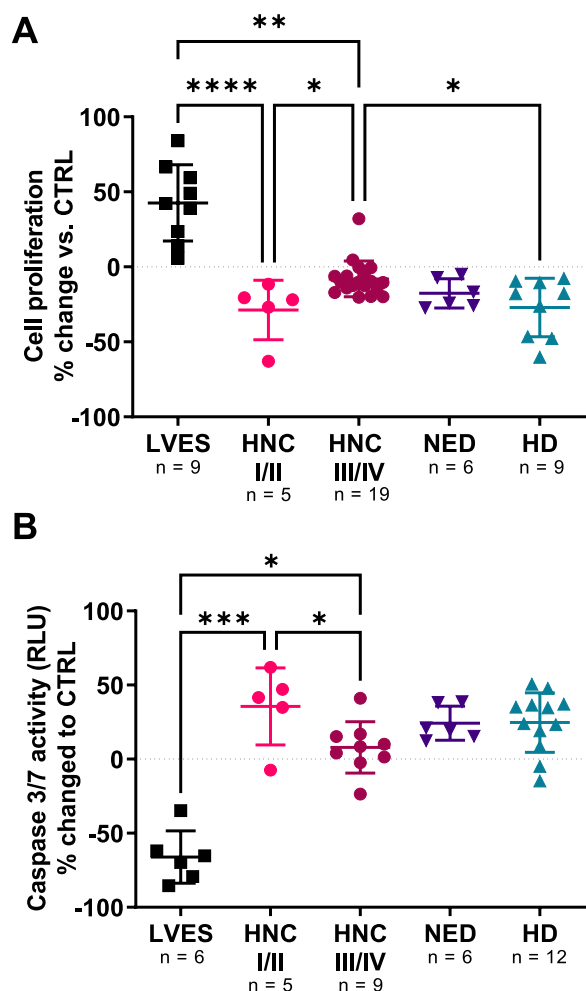


Fig. 6 Proliferation and apoptosis of HUVECs in the presence of plasma sEVs. HUVECs and plasma sEVs from HNC patients, NED and HDs were co-incubated for 24 h. Proliferation (MTS assay) and apoptosis induction (Caspase3/7) of HUVECs was detected and visualized by scatter plots. The percentage changes compared to the PBS control (dotted line) after stimulation for 24 h is shown. The plots of the **A** MTS Assay and **B** Caspase-Glo 3/7 assay show the inhibition of proliferation and apoptosis induction by sEVs in relation to the disease activity and tumor stage of the HNC patients. * $p < 0.05$; ** $p < 0.01$; *** $p < 0.001$; **** $p < 0.0001$

angiogenin, some of which are also found in sEV preparations (Lamalice et al. 2007). Tubulogenesis is a complex process involving migration, proliferation, lumen formation and sprouting of ECs (Geudens and Gerhardt 2011), but without stabilization, the immature capillaries rapidly become apoptotic and regress (Benjamin et al. 1998). Here, plasma sEVs seem to affect tubulogenesis already in the growth phase. In vitro, MMP-9 expression was crucial for cell migration and tube formation in microvascular ECs (Jadhav et al. 2004) and MMP-9 treatment substantially increased tube formation in HUVECs

(Santhekadur et al. 2012). Therefore, the elevated levels of MMP-9 in HNC sEVs and internalization by ECs might contribute to the less pronounced anti-angiogenic activity, while the high levels of thrombospondin-1 in sEV preparations might be responsible for the increased apoptosis.

Recently, studies have also pointed to a central role of immunosuppressive adenosine in tumor angiogenesis (Ludwig et al. 2020a, 2020b). Its production is stimulated by increased CD39 and CD73 cargo on HNC cell line sEVs, but also on plasma-derived sEVs, possibly contributing to their effect on ECs (Ludwig et al. 2017).

To date, most functional studies have focused on the role of sEVs derived from tumor cell lines showing a pro-angiogenic effect on endothelial cells (i.e. glioblastoma (Skog et al. 2008; Lang et al. 2017), breast cancer (Maji et al. 2017; Eichelser et al. 2014) and colorectal cancer (Huang and Feng 2017) but also HNC (Ludwig et al. 2018)). Of note, sEVs are secreted by all cell types. Consequently, plasma contains a mixture of sEVs from various cells, including immune cells, platelets, erythrocytes and ECs. Some of these cells secrete sEVs with pro- or anti-angiogenic functions depending on the stimulus for vesicle release (Todorova et al. 2017; Yang et al. 2008; Ramakrishnan et al. 2016). There have been some controversial studies on sEVs derived from serum of cancer patients that promoted angiogenesis and showed no inhibitory effect on endothelial cells (Hsu et al. 2017; O'Brien et al. 2013). However, the use of serum as an sEV source leads to a higher amount of platelet-associated-proteins and EVs (Zhang et al. 2012) that were previously shown to also have pro-angiogenic properties and might limit these results (Kim et al. 2004).

Possibly, advanced HNC might secrete elevated levels of tumor-derived sEVs that stimulate angiogenesis in comparison to HD and NED, in which anti-angiogenic sEVs prevail.

To verify the hypothesis of a stronger pro-angiogenic effect of TEVs within HNC patients' sEVs, bead-based separation techniques of tumor-derived sEVs from plasma as described by others could be employed for future studies (Beccard et al. 2020; Theodoraki et al. 2018; Benecke et al. 2022) and would provide a deeper insight into the angiogenic potential of TEVs and sEVs in general.

The preparation of sEVs by size exclusion chromatography provides a high yield of high-quality vesicles (Hong et al. 2016). However, functional analyses of plasma sEVs requires a fresh preparation of the specimens to provide reliable results (Muller et al. 2014). In some experiments within this study, the performance of the experiments required high protein amounts and several repetitions to show reproducible and reliable results, which resulted

in varying numbers of patients and HD in the different experiments.

Nevertheless, the following conclusions can be drawn from this study: In summary, plasma sEVs from HNC patients modulate angiogenesis in a stage-dependent manner. Since the greatest functional differences between HD and HNC are observed at advanced stages, analysis of the signaling pathways and proteomic profiles responsible for these differences could lead to the discovery of novel prognostic biomarkers for HNC. Because the clinical utility of angiogenesis inhibitors in the treatment of HNC patients remains unclear and some are associated with increased toxicity (e.g. bevacizumab) (Argiris et al. 2019), targeting sEV uptake by recipient endothelial cells or sEV release by tumor cells may represent an alternative option. Further studies are needed to expand the understanding of sEVs in angiogenesis.

Conclusions

The pro-angiogenic properties of plasma sEVs are increasing with higher disease activity and tumor stages, which might reflect a higher abundance of tumor-derived sEVs (TEV) in patients with advanced-stage HNC. Ultimately, targeting TEV and sEV-mediated angiogenesis might serve as a promising tool for cancer therapy in the future.

Abbreviations

ApoA1	Apolipoprotein A1
BCA	Bicinchoninic acid
bFGF	Basic fibroblast growth factor
BSA	Bovine serum albumin
DAPI	4',6-Diamidino-2-phenylindol
DPPIV	Dipeptidyl peptidase IV
EC	Endothelial cell
ECM	Extracellular matrix
EGF	Epidermal growth factor
EV	Extracellular vesicle
FGF	Fibroblast growth factor
Grp94	Glucose-regulated protein 94
HD	Healthy donor
HNC	Head and neck cancer
HNSCC	Head and neck squamous cell carcinoma
HRP	Horseradish peroxidase
HUVEC	Human umbilical vein endothelial cells
IGFBP	Insulin-like growth factor-binding protein
IL-8	Interleukin 8
LDEV	Lactate dehydrogenase elevating virus
LVES	Larger vessel endothelial supplement
MMP-8	Matrixmetalloproteinase 8
MMP-9	Matrixmetalloproteinase 9
MTS	(3-(4,5-Dimethylthiazol-2-yl)-5-(3-carboxymethoxyphenyl)-2-(4-sulfophenyl)-2H-tetrazolium)
NED	No evident disease
NTA	Nanoparticle tracking analysis
PBS	Phosphate buffered saline
PD-1	Programmed cell death protein 1
PDGF	Platelet-derived growth factor
RT	Room temperature
sEV	Small extracellular vesicle

TEM	Transmission electron microscopy
TEV	Tumor-derived sEVs
TGF- β	Transforming growth factor β
TME	Tumor microenvironment
TSG101	Tumor susceptibility gene 101 protein
UICC	Union for International Cancer Control
uPA	Urokinase-type Plasminogen Activator
VEGF	Vascular Endothelial Growth Factor

Supplementary Information

The online version contains supplementary material available at <https://doi.org/10.1186/s10020-023-00659-w>.

Additional file 1: Table S1. Mean pixel density of spots on Antibody Array.

Additional file 2. Fig. S1. Original Western blot images for sEV characterization.

Additional file 3. Fig. S2. Titration curve for optimal sEV concentration used for the MTS assay.

Additional file 4. Fig. S3. Correlation of clinical factors with the wound healing effect of sEVs.

Additional file 5. Fig. S4. Correlation of clinical factors with the effect of sEVs on tubulogenesis.

Additional file 6. Fig. S5. Correlation of clinical factors with the effect of sEVs on EC proliferation.

Additional file 7. Fig. S6. Correlation of clinical factors with apoptosis induction of sEVs.

Acknowledgements

The authors thank Dr. Stefan Hillmer and Dr. Charlotta Funaya from the Electron Microscopy Core Facility for the acquisition of TEM micrographs and acknowledge the support of the Live Cell Imaging Mannheim (LIMa) Core Facility.

Author contributions

Conception & design: LT, JS, SL—Data acquisition: LT, MT, KN—Data analysis: LT, CW—Data interpretation: LT, SL, M-NT, JJ, ES, FJ—Manuscript draft: LT, SL—Manuscript review: AA, M-NT, NR, JJ, AL. All authors read and approved the final manuscript.

Funding

Open Access funding enabled and organized by Projekt DEAL. This study was funded by the German Research Foundation (DFG) and the Foundation for Cancer and Scarlet Fever Research. For the publication fee we acknowledge financial support by Deutsche Forschungsgemeinschaft within the funding programme „Open Access Publikationskosten“ as well as by Heidelberg University.

Availability of data and materials

The participants of this study did not give written consent for their data to be shared publicly, so due to the sensitive nature of the research supporting data is not available.

Declarations

Ethics approval and consent to participate

The study was approved by the local ethics committee (2021-552 und 2019-697N) and all participants signed informed consent before study inclusion.

Consent for publication

All authors read and approved the final manuscript.

Competing interests

The authors declare that they have no competing interests.

Author details

¹Department of Otorhinolaryngology, Head and Neck Surgery, Medical Faculty Mannheim, University Hospital Mannheim, University of Heidelberg, Mannheim, Germany. ²Translational Oncology, Department of Otorhinolaryngology, University Hospital Essen, University of Duisburg-Essen, Essen, Germany. ³Department of Otorhinolaryngology, Head and Neck Surgery, Ulm University Medical Center, Ulm, Germany. ⁴Department of Urology and Uro-surgery, Medical Faculty Mannheim, University Hospital Mannheim, University of Heidelberg, Mannheim, Germany. ⁵Department of Medical Statistics and Biomathematics, Medical Faculty Mannheim, University Hospital Mannheim, University of Heidelberg, Mannheim, Germany.

Received: 19 January 2023 Accepted: 26 April 2023

Published online: 24 May 2023

References

- Adams RH, Alitalo K. Molecular regulation of angiogenesis and lymphangiogenesis. *Nat Rev Mol Cell Biol.* 2007;8:464–78. <https://doi.org/10.1038/nrm2183>.
- Argiris A, Li S, Sawides P, Ohr JP, Gilbert J, Levine MA, et al. Phase III randomized trial of chemotherapy with or without bevacizumab in patients with recurrent or metastatic head and neck cancer. *J Clin Oncol.* 2019;37:3266–74. <https://doi.org/10.1200/JCO.19.00555>.
- Beccard IJ, Hofmann L, Schroeder JC, Ludwig S, Laban S, Brunner C, et al. Immune suppressive effects of plasma-derived exosome populations in head and neck cancer. *Cancers.* 2020. <https://doi.org/10.3390/cancers12071997>.
- Benecke L, Chiang DM, Ebnoether E, Pfaffl MW, Muller L. Isolation and analysis of tumor-derived extracellular vesicles from head and neck squamous cell carcinoma plasma by galectin-based glycan recognition particles. *Int J Oncol.* 2022. <https://doi.org/10.3892/ijo.2022.5423>.
- Benjamin LE, Hemo I, Keshet E. A plasticity window for blood vessel remodeling is defined by pericyte coverage of the preformed endothelial network and is regulated by PDGF-B and VEGF. *Development.* 1998;125:1591–8. <https://doi.org/10.1242/dev.125.9.1591>.
- Bergers G, Benjamin LE. Tumorigenesis and the angiogenic switch. *Nat Rev Cancer.* 2003;3:401–10. <https://doi.org/10.1038/nrc1093>.
- Bergers G, Brekken R, McMahon G, Vu TH, Itoh T, Tamaki K, et al. Matrix metalloproteinase-9 triggers the angiogenic switch during carcinogenesis. *Nat Cell Biol.* 2000;2:737–44. <https://doi.org/10.1038/35036374>.
- Carpentier G. Angiogenesis analyzer for imageJ. 2012. <http://image.bio.methods.free.fr/ImageJ/?Angiogenesis-Analyzer-for-ImageJ&lang=en>. Accessed 7 May 2021.
- Dawson DW, Volpert OV, Gillis P, Crawford SE, Xu H, Benedict W, Bouck NP. Pigment epithelium-derived factor: a potent inhibitor of angiogenesis. *Science.* 1999;285:245–8. <https://doi.org/10.1126/science.285.5425.245>.
- de Vicente JC, Fresno MF, Villalain L, Vega JA, Hernández VG. Expression and clinical significance of matrix metalloproteinase-2 and matrix metalloproteinase-9 in oral squamous cell carcinoma. *Oral Oncol.* 2005;41:283–93. <https://doi.org/10.1016/j.oraloncology.2004.08.013>.
- Eichelscher C, Stückerath I, Müller V, Milde-Langosch K, Wikman H, Pantel K, Schwarzenbach H. Increased serum levels of circulating exosomal microRNA-373 in receptor-negative breast cancer patients. *Oncotarget.* 2014;5:9650–63. <https://doi.org/10.18632/oncotarget.2520>.
- Ferris RL, Blumenschein G, Fayette J, Guigay J, Colevas AD, Licitra L, et al. Nivolumab for recurrent squamous-cell carcinoma of the head and neck. *N Engl J Med.* 2016;375:1856–67. <https://doi.org/10.1056/NEJMoa1602252>.
- Geudens I, Gerhardt H. Coordinating cell behaviour during blood vessel formation. *Development.* 2011;138:4569–83. <https://doi.org/10.1242/dev.062323>.
- Hanahan D, Weinberg RA. Hallmarks of cancer: the next generation. *Cell.* 2011;144:646–74. <https://doi.org/10.1016/j.cell.2011.02.013>.
- Hong C-S, Funk S, Muller L, Boyiadzis M, Whiteside TL. Isolation of biologically active and morphologically intact exosomes from plasma of patients with cancer. *J Extracell Vesicles.* 2016;5:29289. <https://doi.org/10.3402/jev.v5.29289>.
- Hsu Y-L, Hung J-Y, Chang W-A, Lin Y-S, Pan Y-C, Tsai P-H, et al. Hypoxic lung cancer-secreted exosomal miR-23a increased angiogenesis and vascular permeability by targeting prolyl hydroxylase and tight junction protein ZO-1. *Oncogene.* 2017;36:4929–42. <https://doi.org/10.1038/ncr.2017.105>.
- Huang Z, Feng Y. Exosomes derived from hypoxic colorectal cancer cells promote angiogenesis through wnt4-induced β -catenin signaling in endothelial cells. *Oncol Res.* 2017;25:651–61. <https://doi.org/10.3727/096504016X14752792816791>.
- Jablonska J, Rist M, Spyra I, Tengler L, Domnich M, Kansy B, et al. Evaluation of immunoregulatory biomarkers on plasma small extracellular vesicles for disease progression and early therapeutic response in head and neck cancer. *Cells.* 2022. <https://doi.org/10.3390/cells11050902>.
- Jadhav U, Chigurupati S, Lakka S, Mohanam S. Inhibition of matrix metalloproteinase-9 reduces in vitro invasion and angiogenesis in human microvascular endothelial cells. *Int J Oncol.* 2004. <https://doi.org/10.3892/ijo.25.5.1407>.
- Jia H, Zhang Q, Liu F, Zhou D. Prognostic value of MMP-2 for patients with ovarian epithelial carcinoma: a systematic review and meta-analysis. *Arch Gynecol Obstet.* 2017;295:689–96. <https://doi.org/10.1007/s00404-016-4257-9>.
- Johnson DE, Burtress B, Leemans CR, Lui VVY, Bauman JE, Grandis JR. Head and neck squamous cell carcinoma. *Nat Rev Dis Primers.* 2020;6:92. <https://doi.org/10.1038/s41572-020-00224-3>.
- Kim HK, Song KS, Chung J-H, Lee KR, Lee S-N. Platelet microparticles induce angiogenesis in vitro. *Br J Haematol.* 2004;124:376–84. <https://doi.org/10.1046/j.1365-2141.2003.04773.x>.
- Lamalace L, Le Boeuf F, Huot J. Endothelial cell migration during angiogenesis. *Circ Res.* 2007;100:782–94. <https://doi.org/10.1161/01.RES.0000259593.07661.1e>.
- Lang H-L, Hu G-W, Zhang B, Kuang W, Chen Y, Wu L, Xu G-H. Glioma cells enhance angiogenesis and inhibit endothelial cell apoptosis through the release of exosomes that contain long non-coding RNA CCAT2. *Oncol Rep.* 2017;38:785–98. <https://doi.org/10.3892/or.2017.5742>.
- Lawler PR, Lawler J. Molecular basis for the regulation of angiogenesis by thrombospondin-1 and -2. *Cold Spring Harb Perspect Med.* 2012;2:a006627. <https://doi.org/10.1101/cshperspect.a006627>.
- Liu CY, Battaglia M, Lee SH, Sun Q-H, Aster RH, Visentin GP. Platelet factor 4 differentially modulates CD4+CD25+ (regulatory) versus CD4+CD25- (nonregulatory) T cells. *J Immunol.* 2005;174:2680–6. <https://doi.org/10.4049/jimmunol.174.5.2680>.
- Liu Z, Li L, Yang Z, Luo W, Li X, Yang H, et al. Increased expression of MMP9 is correlated with poor prognosis of nasopharyngeal carcinoma. *BMC Cancer.* 2010;10:270. <https://doi.org/10.1186/1471-2407-10-270>.
- Liu Z, Wen J, Hu F, Wang J, Hu C, Zhang W. Thrombospondin-1 induced programmed death-ligand 1-mediated immunosuppression by activating the STAT3 pathway in osteosarcoma. *Cancer Sci.* 2022;113:432–45. <https://doi.org/10.1111/cas.15237>.
- Ludwig S, Floros T, Theodoraki M-N, Hong C-S, Jackson EK, Lang S, Whiteside TL. Suppression of lymphocyte functions by plasma exosomes correlates with disease activity in patients with head and neck cancer. *Clin Cancer Res.* 2017;23:4843–54. <https://doi.org/10.1158/1078-0432.CCR-16-2819>.
- Ludwig N, Yerneni SS, Razzo BM, Whiteside TL. Exosomes from HNSCC promote angiogenesis through reprogramming of endothelial cells. *Mol Cancer Res.* 2018;16:1798–808. <https://doi.org/10.1158/1541-7786.MCR-18-0358>.
- Ludwig N, Yerneni SS, Azambuja JH, Gillespie DG, Menshikova EV, Jackson EK, Whiteside TL. Tumor-derived exosomes promote angiogenesis via adenosine A2B receptor signaling. *Angiogenesis.* 2020a;23:599–610. <https://doi.org/10.1007/s10456-020-09728-8>.
- Ludwig N, Jackson EK, Whiteside TL. Role of exosome-associated adenosine in promoting angiogenesis. *Vessel plus.* 2020b. <https://doi.org/10.20517/2574-1209.2019.37>.
- Maji S, Chaudhary P, Akopova I, Nguyen PM, Hare RJ, Gryczynski I, Vishwanatha JK. Exosomal annexin II promotes angiogenesis and breast cancer metastasis. *Mol Cancer Res.* 2017;15:93–105. <https://doi.org/10.1158/1541-7786.MCR-16-0163>.
- Miao C, Liang C, Zhu J, Xu A, Zhao K, Hua Y, et al. Prognostic role of matrix metalloproteinases in bladder carcinoma: a systematic review and meta-analysis. *Oncotarget.* 2017;8:32309–21. <https://doi.org/10.18632/oncotarget.15907>.
- Muller L, Hong C-S, Stolz DB, Watkins SC, Whiteside TL. Isolation of biologically active exosomes from human plasma. *J Immunol Methods.* 2014;411:55–65. <https://doi.org/10.1016/j.jim.2014.06.007>.

- Notari L, Miller A, Martínez A, Amaral J, Ju M, Robinson G, et al. Pigment epithelium-derived factor is a substrate for matrix metalloproteinase type 2 and type 9: implications for downregulation in hypoxia. *Invest Ophthalmol Vis Sci.* 2005;46:2736–47. <https://doi.org/10.1167/iovs.04-1489>.
- O'Brien K, Rani S, Corcoran C, Wallace R, Hughes L, Friel AM, et al. Exosomes from triple-negative breast cancer cells can transfer phenotypic traits representing their cells of origin to secondary cells. *Eur J Cancer.* 2013;49:1845–59. <https://doi.org/10.1016/j.ejca.2013.01.017>.
- Pilatova K, Greplova K, Demlova R, Bencsikova B, Klement GL, Zdrzilova-Dubská L. Role of platelet chemokines, PF-4 and CTAP-III, in cancer biology. *J Hematol Oncol.* 2013;6:42. <https://doi.org/10.1186/1756-8722-6-42>.
- Pužar Dominkuš P, Stenovc M, Sitar S, Lasič E, Zorec R, Plemenitaš A, et al. PKH26 labeling of extracellular vesicles: Characterization and cellular internalization of contaminating PKH26 nanoparticles. *Biochim Biophys Acta Biomembr.* 2018;1860:1350–61. <https://doi.org/10.1016/j.bbamem.2018.03.013>.
- Ramakrishnan DP, Hajj-Ali RA, Chen Y, Silverstein RL. Extracellular vesicles activate a CD36-dependent signaling pathway to inhibit microvascular endothelial cell migration and tube formation. *Arterioscler Thromb Vasc Biol.* 2016;36:534–44. <https://doi.org/10.1161/ATVBAHA.115.307085>.
- Santhekadur PK, Gredler R, Chen D, Siddiq A, Shen X-N, Das SK, et al. Late SV40 factor (LSF) enhances angiogenesis by transcriptionally up-regulating matrix metalloproteinase-9 (MMP-9). *J Biol Chem.* 2012;287:3425–32. <https://doi.org/10.1074/jbc.M111.298976>.
- Skog J, Würdinger T, van Rijn S, Meijer DH, Gainche L, Sena-Esteves M, et al. Glioblastoma microvesicles transport RNA and proteins that promote tumour growth and provide diagnostic biomarkers. *Nat Cell Biol.* 2008;10:1470–6. <https://doi.org/10.1038/ncb1800>.
- Sung H, Ferlay J, Siegel RL, Laversanne M, Soerjomataram I, Jemal A, Bray F. Global cancer statistics 2020: GLOBOCAN estimates of incidence and mortality worldwide for 36 cancers in 185 countries. *CA Cancer J Clin.* 2021;71:209–49. <https://doi.org/10.3322/caac.21660>.
- Theodoraki M-N, Hoffmann TK, Whiteside TL. Separation of plasma-derived exosomes into CD3(+) and CD3(-) fractions allows for association of immune cell and tumour cell markers with disease activity in HNSCC patients. *Clin Exp Immunol.* 2018;192:271–83. <https://doi.org/10.1111/cei.13113>.
- Todorova D, Simoncini S, Lacroix R, Sabatier F, Dignat-George F. Extracellular vesicles in angiogenesis. *Circ Res.* 2017;120:1658–73. <https://doi.org/10.1161/CIRCRESAHA.117.309681>.
- Whiteside TL. Tumor-derived exosomes and their role in cancer progression. *Adv Clin Chem.* 2016;74:103–41. <https://doi.org/10.1016/bs.acc.2015.12.005>.
- Whiteside TL. Head and neck carcinoma immunotherapy: facts and hopes. *Clin Cancer Res.* 2018;24:6–13. <https://doi.org/10.1158/1078-0432.CCR-17-1261>.
- Yang C, Mwaikambo BR, Zhu T, Gagnon C, Lafleur J, Seshadri S, et al. Lymphocytic microparticles inhibit angiogenesis by stimulating oxidative stress and negatively regulating VEGF-induced pathways. *Am J Physiol Regul Integr Comp Physiol.* 2008;294:R467–76. <https://doi.org/10.1152/ajpregu.00432.2007>.
- Yeon JH, Jeong HE, Seo H, Cho S, Kim K, Na D, et al. Cancer-derived exosomes trigger endothelial to mesenchymal transition followed by the induction of cancer-associated fibroblasts. *Acta Biomater.* 2018;76:146–53. <https://doi.org/10.1016/j.actbio.2018.07.001>.
- Zhang X, Takeuchi T, Takeda A, Mochizuki H, Nagai Y. Comparison of serum and plasma as a source of blood extracellular vesicles: increased levels of platelet-derived particles in serum extracellular vesicle fractions alter content profiles from plasma extracellular vesicle fractions. *PLoS ONE.* 2022;17:e0270634. <https://doi.org/10.1371/journal.pone.0270634>.
- Zhao Y, Qiao X, Wang L, Tan TK, Zhao H, Zhang Y, et al. Matrix metalloproteinase 9 induces endothelial-mesenchymal transition via Notch activation in human kidney glomerular endothelial cells. *BMC Cell Biol.* 2016;17:21. <https://doi.org/10.1186/s12860-016-0101-0>.

Publisher's Note

Springer Nature remains neutral with regard to jurisdictional claims in published maps and institutional affiliations.

Ready to submit your research? Choose BMC and benefit from:

- fast, convenient online submission
- thorough peer review by experienced researchers in your field
- rapid publication on acceptance
- support for research data, including large and complex data types
- gold Open Access which fosters wider collaboration and increased citations
- maximum visibility for your research: over 100M website views per year

At BMC, research is always in progress.

Learn more biomedcentral.com/submissions

